

Regulated NiCu Cycles with the New $^{57}\text{Cu}(\text{p},\gamma)^{58}\text{Zn}$ Reaction Rate and the Influence on Type-I X-Ray Bursts: GS 1826–24 Clocked Burster

Yi Hua Lam^{1,2,}, Ning Lu^{1,2,3,**}, Alexander Heger^{4,5,6,7,***}, Adam Michael Jacobs^{7,8}, Nadezda A. Smirnova⁹, Teresa Kurtukian Nieto⁹, Zac Johnston^{7,8}, and Shigeru Kubono^{10,11}*

¹Institute of Modern Physics, Chinese Academy of Sciences, Lanzhou 730000, China

²School of Nuclear Science and Technology, University of Chinese Academy of Sciences, Beijing 100049, China

³School of Nuclear Science and Technology, Lanzhou University, Lanzhou 730000, China

⁴School of Physics and Astronomy, Monash University, Victoria 3800, Australia

⁵OzGrav-Monash – MOCA, School of Physics and Astronomy, Monash University, VIC 3800, Australia

⁶Center of Excellence for Astrophysics in Three Dimensions (ASTRO-3D), Australia

⁷The Joint Institute for Nuclear Astrophysics, Michigan State University, East Lansing, MI 48824, USA

⁸Department of Physics and Astronomy, Michigan State University, East Lansing, MI 48824, USA

⁹CENBG, CNRS/IN2P3 and University of Bordeaux, Chemin du Solarium, 33175 Gradignan cedex, France

¹⁰RIKEN Nishina Center, 2-1 Hirosawa, Wako, Saitama 351-0198, Japan

¹¹Center for Nuclear Study, University of Tokyo, 2-1 Hirosawa, Wako, Saitama 351-0198, Japan

Abstract. In Type-I X-ray bursts (XRBs), the rapid-proton capture (rp-) process passes through the NiCu and ZnGa cycles before reaching the region above Ge and Se isotopes that hydrogen burning actively powers the XRBs. The sensitivity study performed by Cyburt *et al.* [1] shows that the $^{57}\text{Cu}(\text{p},\gamma)^{58}\text{Zn}$ reaction in the NiCu cycles is the fifth most important rp-reaction influencing the burst light curves. Langer *et al.* [2] precisely measured some low-lying energy levels of ^{58}Zn to deduce the $^{57}\text{Cu}(\text{p},\gamma)^{58}\text{Zn}$ reaction rate. Nevertheless, the order of the 1_1^+ and 2_3^+ resonance states that dominate at $0.2 \lesssim T(\text{GK}) \lesssim 0.8$ is not confirmed. The 1_2^+ resonance state, which dominates at the XRB sensitive temperature regime $0.8 \lesssim T(\text{GK}) \lesssim 2$ was not detected. Using isobaric-multiplet-mass equation (IMME), we estimate the order of the 1_1^+ and 2_3^+ resonance states and estimate the lower limit of the 1_2^+ resonance energy. We then determine the $^{57}\text{Cu}(\text{p},\gamma)^{58}\text{Zn}$ reaction rate using the full *pf*-model space shell model calculations. The new rate is up to a factor of four lower than the Forstner *et al.* [3] rate recommended by JINA REACLIBv2.2. Using the present $^{57}\text{Cu}(\text{p},\gamma)^{58}\text{Zn}$, the latest $^{56}\text{Ni}(\text{p},\gamma)^{57}\text{Cu}$ and $^{55}\text{Ni}(\text{p},\gamma)^{56}\text{Cu}$ reaction rates, and 1D implicit hydrodynamic KEPLER code, we model the thermonuclear XRBs of the clocked burster GS 1826–24. We find that the new rates regulate the reaction flow in the NiCu cycles and strongly influence the burst-ash composition. The $^{59}\text{Cu}(\text{p},\alpha)^{56}\text{Ni}$ and $^{59}\text{Cu}(\text{p},\gamma)^{60}\text{Zn}$ reactions suppress the influence of the $^{57}\text{Cu}(\text{p},\gamma)^{58}\text{Zn}$ reaction. They strongly diminish the impact of the nuclear reaction flow that bypasses the ^{56}Ni waiting point induced by the $^{55}\text{Ni}(\text{p},\gamma)^{56}\text{Cu}$ reaction on burst light curve.

The $^{57}\text{Cu}(\text{p},\gamma)^{58}\text{Zn}$ reaction is the fifth most influential (p,γ) reaction that affects the light curve of GS 1826–24, the clocked burster [4], as found by Cyburt *et al.* [1]. Langer *et al.*

*e-mail: lamyihua@impcas.ac.cn

**Presenter

***e-mail: alexander.heger@monash.edu

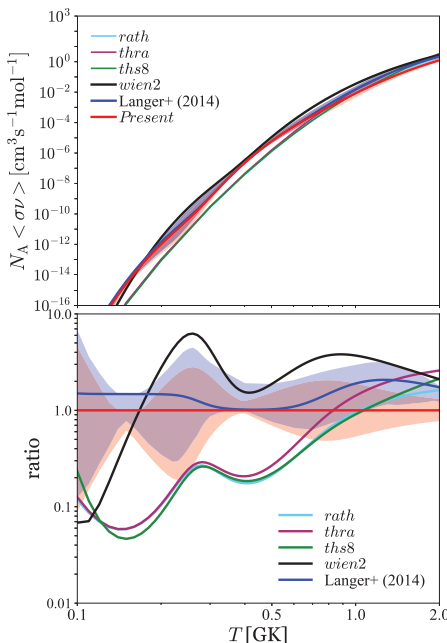


Figure 1. Top Panel: The *Present* and Langer *et al.* [2] $^{57}\text{Cu}(\text{p},\gamma)^{58}\text{Zn}$ thermonuclear reaction rates, and available reaction rates compiled in to JINA REACLIB v2.2: *rath*, *thra*, *ths8*, and *wien2* [3], the rate recommended by JINA REACLIB v2.2. All available rates of REACLIB v2.2 use the ^{58}Zn proton threshold, $S_p(^{58}\text{Zn}) = 2.277$ MeV. Bottom Panel: The comparison of the *Present* rate with Langer *et al.* and all available reaction rates of REACLIB v2.2. The uncertainty of the *Present* rate (red zone) folds the uncertainties from the $S_p(^{58}\text{Zn})$ and nuclear structure. The uncertainty of Langer *et al.* rate is indicated as blue zone. The rates of *rath*, *thra*, and *ths8* based on the Hauser-Feshbach statistical model are very close to one another from 0.1 to 2.0 GK, and they are lower than the *Present* rate up to one order of magnitude at temperature $T \lesssim 0.9$ GK. The *Present* rate is up to a factor of two lower than Langer *et al.* rate from 0.8 to 2 GK covering the typical maximum temperature of accreted envelope of the GS 1826–24 burster, and up to a factor of four lower than the *wien2* rate [3].

[2] experimentally confirmed some low-lying excited states of ^{58}Zn , which are resonance states dominantly contribute to the $^{57}\text{Cu}(\text{p},\gamma)^{58}\text{Zn}$ reaction rate. The order of the dominant resonance states, 1_1^+ and 2_3^+ , that they precisely measured was, however, unconfirmed. The 1_2^+ resonance state, one of the dominant resonances sensitive to the clocked burst temperature regime, $0.8 \lesssim T(\text{GK}) \lesssim 2$, was not detected.

In the present study, we first compare the theoretical and experimental IMME c coefficients for the $A = 58$, isospin $I = 1$ multiplets to obtain the root-mean-square (rms) deviation value 22 keV as the theoretical uncertainty. Then, we study and propose the most plausible order of the 2_3^+ and 1_1^+ states based on the $A = 58$, $I = 1$ multiplets of ^{58}Zn , ^{58}Cu , and ^{58}Ni . We then use IMME to estimate the lowest limit energy of the 1_2^+ state (3.664 ± 0.022 MeV). The corresponding resonance energy is 1.384 MeV. This is 329 keV higher than the direct estimation of shell-model calculation by Langer *et al.* [2]. The contribution of the 1_2^+ resonance state reduces by about one order of magnitude, reducing the total reaction rate in the temperature regime $0.8 \lesssim T(\text{GK}) \lesssim 2$. With the presently deduced nuclear structure information, we use the full *pf*-model space shell model calculations with GXPF1A interaction [5] to construct the *Present* $^{57}\text{Cu}(\text{p},\gamma)^{58}\text{Zn}$ reaction rate for the typical XRB temperature range, in particular, the temperature regime of $0.8 \lesssim T(\text{GK}) \lesssim 1.6$ relevant to the GS 1826–24 burster. The comparison of the *Present* rate with Langer *et al.* rate and with other reaction rates compiled into JINA REACLIB v2.2 [6] is shown in Fig. 1.

Using the GS 1826–24 model obtained from KEPLER, we construct three XRB models based on each combination of reaction rates: (1) the *Present* $^{57}\text{Cu}(\text{p},\gamma)^{58}\text{Zn}$, *et al.* Kahl [7] $^{56}\text{Ni}(\text{p},\gamma)^{57}\text{Cu}$, and Valverde [8] $^{55}\text{Ni}(\text{p},\gamma)^{56}\text{Cu}$, (2) Langer [2] $^{57}\text{Cu}(\text{p},\gamma)^{58}\text{Zn}$, Kahl [7] $^{56}\text{Ni}(\text{p},\gamma)^{57}\text{Cu}$, and Valverde [8] $^{55}\text{Ni}(\text{p},\gamma)^{56}\text{Cu}$, and (3) *wien2* [3] $^{57}\text{Cu}(\text{p},\gamma)^{58}\text{Zn}$. These (1), (2), and (3) combinations are labeled as *Present*[§], *Present*[◊], and *baseline* models, respectively.

We remark that the observed burst tail end of *Epoch Jun 1998* of the GS 1826–24 burster is closely reproduced by the *Present*[§], *Present*[◊], and *baseline* models (Fig. 5 of Ref. [9]). Figure 2 shows the burst-ash composition at the burst tail end produced by three models. Using

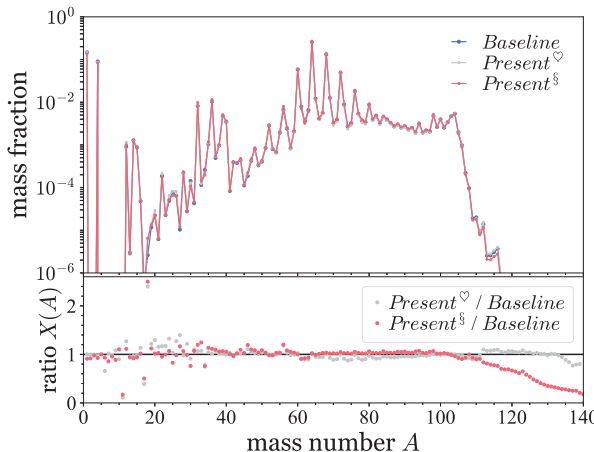


Figure 2. The averaged mass fractions for each mass number at burst tail end when $t \approx 180$ s after the burst peak. The GS 1826–24 model from Jacobs *et al.* [10] is the adjusted to reproduce the recurrence time of *Epoch Jun 1998*. The model uses JINA REACLIB v2.2. and is named as *baseline* model. The *Present^v* (or *Present^s*) model adopts the same astrophysical configurations of *baseline* but implement the *Present* (or Langer *et al.*) $^{57}\text{Cu}(\text{p},\gamma)^{58}\text{Zn}$, Kahl *et al.* [7] $^{56}\text{Ni}(\text{p},\gamma)^{57}\text{Cu}$ and Valverde *et al.* [8] $^{55}\text{Ni}(\text{p},\gamma)^{56}\text{Cu}$ rates, see text.

the *Present* $^{57}\text{Cu}(\text{p},\gamma)^{58}\text{Zn}$ rate, the production of ^{12}C is reduced by a factor of 0.2, the nuclei with $A = 17$ and 18 breaking out from the hot CNO cycle are affected up to about a factor of 0.5 and 2.5, respectively. The abundances of the daughters of SiP, SCl, and ArK cycles are reduced up to a factor of 0.7. The overall production of ^{56}Ni and its remnant increases up to a factor of 1.2 due to the *correlated influence* between the new $^{56}\text{Ni}(\text{p},\gamma)^{57}\text{Cu}$, $^{57}\text{Cu}(\text{p},\gamma)^{58}\text{Zn}$, and $^{55}\text{Ni}(\text{p},\gamma)^{56}\text{Cu}$ rates. The abundances of nuclei with $A = 64 - 104$ produced by *Present^s* are closer to *baseline* than the ones produced by *Present^v*. Furthermore, the abundances of the nuclei with $A = 105 - 140$ are decreased by up to a factor of 0.2 (red dots in the bottom panel of Fig. 2). Notably, the Langer *et al.* $^{57}\text{Cu}(\text{p},\gamma)^{58}\text{Zn}$ reaction rate produces a different set of burst-ash composition compared to the *Present* $^{57}\text{Cu}(\text{p},\gamma)^{58}\text{Zn}$ rate, especially the nuclei with $A = 20 - 34$; the abundance of the nuclei with $A = 65 - 84$, is reduced by up to a factor of 0.9; and the abundance of the nuclei with $A = 100 - 134$ is closer to *baseline* than the impact suggested by the change to the *Present* $^{57}\text{Cu}(\text{p},\gamma)^{58}\text{Zn}$ reaction rate.

The impact of *Present* $^{57}\text{Cu}(\text{p},\gamma)^{58}\text{Zn}$, new $^{56}\text{Ni}(\text{p},\gamma)^{57}\text{Cu}$ and $^{55}\text{Ni}(\text{p},\gamma)^{56}\text{Cu}$ rates on burst ash composition is due to the cumulative effect of redistributing and reassembling of reaction flows in the NiCu cycles that eventually affects the nucleosyntheses of ^{56}Ni , ^{57}Cu , ^{58}Zn , and nuclei in the ZnGa cycles. A detail analysis of the evolution of the episode of clocked bursts is presented in Ref. [9].

This work was financially supported by the Strategic Priority Research Program of Chinese Academy of Sciences (CAS, Grant Nos. XDB34000000 and XDB34020204) and National Natural Science Foundation of China (No. 11775277), Chinese Academy of Sciences President's International Fellowship Initiative (No. 2019FYM0002), Australian Research Council Centre of Excellence for Gravitational Wave Discovery (OzGrav, No. CE170100004) and for All Sky Astrophysics in 3 Dimensions (ASTRO 3D, No. CE170100013), IN2P3/CNRS, France, Master Project – “Exotic nuclei, fundamental interactions and astrophysics”.

References

- [1] R. H. Cyburt, A. M. Amthor, A. Heger *et al.*, *Astrophys. J.* **55**, 830 (2016).
- [2] C. Langer, F. Montes, A. Aprahamian *et al.*, *Phys. Rev. Lett.* **113**, 032502 (2014).
- [3] O. Forstner, H. Herndl, H. Oberhummer *et al.*, *Phys. Rev. C* **64**, 045801 (2001).
- [4] F. Makino, *IAU Circ.*, No. 4653 (1988).
- [5] M. Honma, T. Otsuka, B. A. Brown *et al.*, *Phys. Rev. C* **69**, 034335 (2004).
- [6] R. H. Cyburt, A. M. Amthor, R. Ferguson *et al.*, *Astrophys. J. Supp.* **189**, 240 (2010).
- [7] D. Kahl, P. J. Woods, T. Poxon-Pearson, *et al.*, *Phys. Lett. B* **797**, 134803 (2019).
- [8] A. A. Valverde, M. Brodeur, G. Bollen *et al.*, *Phys. Rev. Lett.* **123**, 239905E (2019).
- [9] Y. H. Lam, N. Lu, A. Heger *et al.*, [arXiv:2107.11552](https://arxiv.org/abs/2107.11552).
- [10] J. M. Jacobs, A. Heger *et al.*, *Burst Environment, Reactions and Numerical Modelling Workshop (BERN18)*, 11 – 15 Jun, 2018, Monash Prato Centre, Tuscany, Italy.